Design and Fabrication of a Micro PZT Cantilever Array Actuator for Applications in Fluidic Systems

Hyonse Kim
School of Mechanical and Aerospace Engineering,
Seoul National University, Shinlim-Dong, San 56-1, Kwanak-Gu, Seoul 151-742, Korea
Chihyun In
MEMS Division, DAEWOO Electronics Corp.,
Kasan-dong, Kumchun-gu, Seoul, 153-801, South Korea
Gilho Yoon
Department of Mechanical Engineering, Solid Mechanics, Nils Koppels Allé, DTU,
Building 404, Office 131, DK-2800 Kgs. Lyngby, Denmark
Jongwon Kim*
School of Mechanical and Aerospace Engineering,
Seoul National University, Shinlim-Dong, San 56-1, Kwanak-Gu, Seoul 151-742, Korea

In this article, a micro cantilever array actuated by PZT films is designed and fabricated for micro fluidic systems. The design features for maximizing tip deflections and minimizing fluid leakage are described. The governing equation of the composite PZT cantilever is derived and the actuating behavior predicted. The calculated value of the tip deflection was 15 μm at 5 V. The fabrication process from SIMOX (Separation by oxygen ion implantation) wafer is presented in detail with the PZT film deposition process. The PZT films are characterized by investigating the ferroelectric properties, dielectric constant, and dielectric loss. Tip deflections of 12 μm at 5 V are measured, which agreed well with the predicted value. The 18 μl/s leakage rate of air was observed at a pressure difference of 1000 Pa. Micro cooler is introduced, and its possible application to micro compressor is discussed.

Key Words : Micro Cantilevers Array, PZT Film, Micro Fluidic System

1. Introduction

Lead zirconate titanate (PZT) thin films have become attractive for micro-electromechanical systems (MEMS), such as micro-actuators and micro-sensors, because they have high ferroelectric and piezoelectric characteristics (Itoh et al., 1996; Lee and White, 1998; Yamashita et al., 2002; Nam and Sasaki, 2002; Kim and Koo, 2002; Kim et al., 2004). Flynn et al.(1992) presented piezoelectric micro motors as actuators for micro robots. Koch et al.(1998) reported a micro machined pump based on thick-film piezoelectric actuation, and Kueppers et al.(2002) proposed the integration of sol-gel PZT thin films on silicon cantilever structures for micromirror and microrelay applications.

The coupled electrical and elastic variables of the piezoelectric materials can be expressed in linear equations as follows (Galassi et al., 1999),

$$D=dT+\varepsilon^{T}E \tag{1}$$

$$\varepsilon=s^{E}T+dE \tag{2}$$

* Corresponding Author,
E-mail : jongkim@snu.ac.kr
TEL : +82-2-880-7138; **FAX** : +82-2-883-1513
School of Mechanical and Aerospace Engineering, Seoul National University, Shinlim-Dong, San 56-1, Kwanak-Gu, Seoul 151-742, Korea. (Manuscript **Received** April 19, 2004; **Revised** December 15, 2004)

where D is the dielectric displacement, d the piezoelectric constant, T stress, ε^T dielectric permittivity, $\boldsymbol{E}$ electric field, ε strain and s^E the elastic compliance at constant field, respectively. Considering the symmetry in the poled ceramic, the dielectric displacement and the strain can be rewritten into matrix forms, respectively, using the following tensor,

$$\begin{pmatrix} \varepsilon_1 \\ \varepsilon_2 \\ \varepsilon_3 \\ \varepsilon_4 \\ \varepsilon_5 \\ \varepsilon_6 \\ D_1 \\ D_2 \\ D_3 \end{pmatrix} = \begin{pmatrix} s_{11}^E & s_{12}^E & s_{13}^E & & & & & & d_{31} \\ s_{12}^E & s_{11}^E & s_{13}^E & & & & & & d_{31} \\ s_{13}^E & s_{13}^E & s_{33}^E & & & & & & d_{33} \\ & & & s_{55}^E & & & & & \\ & & & & s_{55}^E & & & & \\ & & & & & s_{66}^E & & & \\ & & & & d_{15} & & \varepsilon_{11}^T & & \\ & & & d_{15} & & & & \varepsilon_{11}^T & \\ d_{31} & d_{31} & d_{33} & & & & & & \varepsilon_{33}^T \end{pmatrix} \begin{pmatrix} T_1 \\ T_2 \\ T_3 \\ T_4 \\ T_5 \\ T_6 \\ \boldsymbol{E}_1 \\ \boldsymbol{E}_2 \\ \boldsymbol{E}_3 \end{pmatrix} \quad (3)$$

This equation can be simplified for the PZT cantilever applications. Generally, PZT cantilever actuators are composed of a top electrode, a PZT layer, and a bottom electrode, as shown in Fig. 1. When an electric field is applied parallel to the remnant polarization, the PZT layer will contract laterally. As a result, the beam will move up by the contraction strain, which is generated by the piezoelectric effect as follows,

$$\varepsilon_1 = d_{31}\boldsymbol{E}_3 \quad (4)$$

where d_{31} is the transverse piezoelectric coefficient.

One of the sensor applications of PZT cantilever is an atomic force microscope (AFM). The general shape of the AFM is pentagonal, whose structure cannot be applied to an actuator for making fluid to flow, due to the large gap around the structure. For controlling fluid flow with minimum leakage, space between the cantilever and the supporting structures should be minimized. High power is also preferable to efficiently control gas or move liquid.

In this study, we fabricated PZT thin film deposited micro cantilever arrays for fluidic systems. Because these arrays were applied to micro fluidic system, they needed to minimize fluidic leakage through the gaps, maximize the deflections of the cantilever tips, and maximize the number of cantilevers in a given area. We designed 117 pairs of PZT cantilevers that provided minimum gaps with their supporting structures to prevent leakage through the cantilevers for a given square area (10×10 mm). To maximize the power, 234 cantilevers in total will vibrate in synchronized motion.

2. Theory

In designing the micro cantilever array, we tried to put as many cantilevers as possible in a given area to meet the requirements. One-hundred and seventeen pairs of cantilevers (234 cantilever in total) could be included in the square (10×10 mm). This is illustrated in Fig. 2. A single unit of micro cantilever array is illustrated in Fig. 3. The main actuator layer is composed of top platinum (Pt), PZT layer, and bottom Pt layer. They are attached to the Poly-Si cantilever. The dimensions of cantilevers are 450 μm long and 300 μm wide. The thickness of the PZT layer is 0.5 μm, top platinum (Pt) electrode 0.15 μm, and

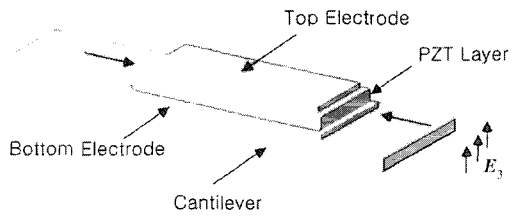

Fig. 1 Schematics of PZT actuator

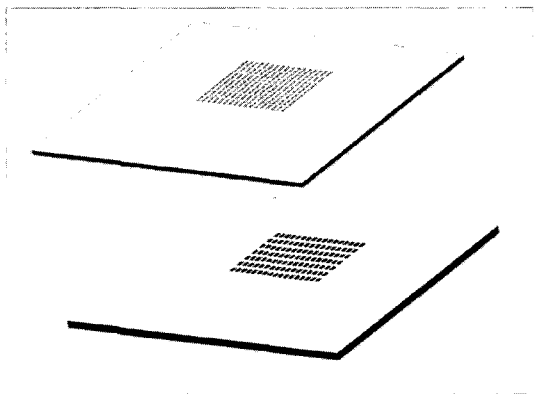

Fig. 2 Schematics of micro cantilevers array of front side view and backside view

bottom Pt electrode 0.15 μm. A thick nitride layer of 0.2 μm thickness acted as an insulator. Ti layer was deposited between the bottom Pt layer and the Poly-Si layer for good adhesion.

Another key point of the design was the minimization of the leakage through the micro cantilevers. Only 4 μm gap was allowed to separate the beam from the supporting parts, as shown in Fig. 4. The value of the gap was the minimum width of the line that could be patterned through photolithography and dry etch processes. So this design is considered to be very efficient for controlling the working fluid.

The other feature of the design is the angled lift-off patterns that connect the top electrodes with bottom power lines. They are connected through the lift-off patterns to supply electric energy. One of difficult fabrication process is the lift-off patterning process because any by-product after etch steps can prohibit clear contact of bridges with bottom lines. This two point contact design confirms good adhesions of the bridges.

The governing equation of the piezoelectric cantilever was derived using forces and equilibrium requirements, relations between forces and strains, and strain compatibility requirements based on the approach by DeVoe et al.(1997) for multimorph deflection. The geometry of the micro cantilever is shown in Figs. 5 and 6. It was divided into two parts: first part with five layers and second part with two layers. In the first part, the second layer from the top is the piezoelectric layer and other layers are elastic. To derive the governing equation, several assumptions were made: the transverse stresses and shear stresses are zero. That is,

$$\varepsilon_2=\varepsilon_3=\varepsilon_4=\varepsilon_5=\varepsilon_6=0 \tag{5}$$

It was also assumed that the radius of curvature when the cantilever is deformed is much larger than the thickness of the beam. Electrostriction can be ignored and residual-stress-induced curvature was negligible.

First, by the equilibrium requirements, the sum of the forces and the moments of the micro cantilever fraction should be zero at equilibrium.

$$\sum F=F_{Top}+F_{PZT}+F_{Bottom}+F_{Oxide}+F_{Poly}=0 \tag{6}$$

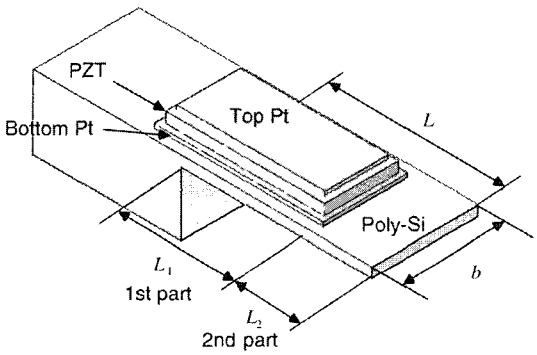

Fig. 3 Schematics of a single unit micro cantilever

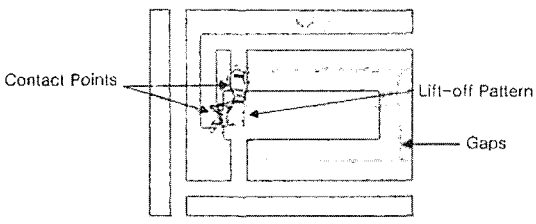

Fig. 4 Microscopy of a single micro cantilever

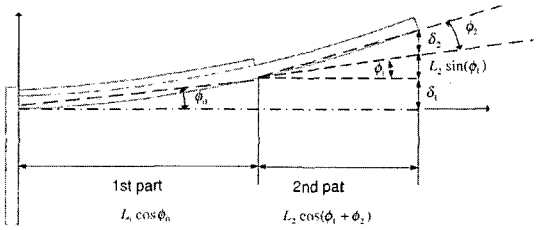

Fig. 5 Mechanical model of the cantilever when it is deformed

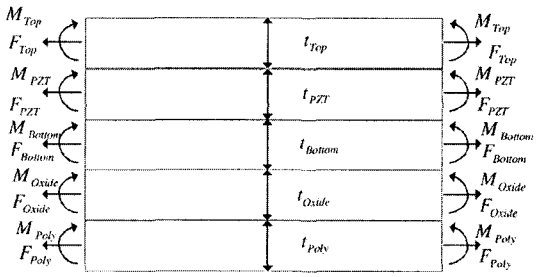

Fig. 6 Fraction of the micro cantilever

$$\begin{aligned}\sum M=&F_{TOP}\left(\frac{t_{Top}}{2}\right)+F_{PZT}\left(t_{Top}+\frac{t_{PZT}}{2}\right)\\&+F_{Bottom}\left(t_{Top}+t_{PZT}+\frac{t_{Bottom}}{2}\right)\\&+F_{Oxide}\left(t_{Top}+t_{PZT}+t_{Bottom}+\frac{t_{Oxide}}{2}\right)\\&+F_{Poly}\left(t_{Top}+t_{PZT}+t_{Bottom}+t_{Oxide}+\frac{t_{Poly}}{2}\right)=0\end{aligned}\tag{7}$$

When linearly elastic beam element is subjected to bending, the radius of curvature r can be expressed by the following equation.

$$\frac{1}{r}=\frac{M}{EI}\tag{8}$$

where E is the modulus of elasticity and I the moment of inertia of the cross-sectional area. Since we assumed that the radius of curvature when the cantilever is deformed is much larger than the thickness of the beam, it is reasonable to assume that the radius of curvature at each layer is same. If we combine Eqs. 7 and 8, we obtain the following equation of the forces and the radius of curvature,

$$\begin{aligned}&\frac{1}{r}[(EI)_{Top}+(EI)_{PZT}+(EI)_{Bottom}+(EI)_{Oxide}+(EI)_{Poly}]\\&=F_{TOP}\left(\frac{t_{Top}}{2}\right)+F_{PZT}\left(t_{Top}+\frac{t_{PZT}}{2}\right)+F_{Bottom}\left(t_{Top}+t_{PZT}+\frac{t_{Bottom}}{2}\right)\\&\quad+F_{Oxide}\left(t_{Top}+t_{PZT}+t_{Bottom}+\frac{t_{Oxide}}{2}\right)\\&\quad+F_{Poly}\left(t_{Top}+t_{PZT}+t_{Bottom}+t_{Oxide}+\frac{t_{Poly}}{2}\right)\end{aligned}\tag{9}$$

For simplicity, the radius of curvature can be written in matrix form as

$$\begin{aligned}\frac{1}{r}=&\frac{1}{[(EI)_{Top}+(EI)_{PZT}+(EI)_{Bottom}+(EI)_{Oxide}+(EI)_{Poly}]}\\&\cdot\left[\left(\frac{t_{Top}}{2}\right)\left(t_{Top}+\frac{t_{PZT}}{2}\right)\left(t_{Top}+t_{PZT}+\frac{t_{Bottom}}{2}\right)\right.\\&\left.\left(t_{Top}+t_{PZT}+t_{Bottom}+\frac{t_{Oxide}}{2}\right)\left(t_{Top}+t_{PZT}+t_{Bottom}+t_{Oxide}+\frac{t_{Poly}}{2}\right)\right]\\&\cdot\begin{bmatrix}F_{Top}\\F_{PZT}\\F_{Bottom}\\F_{Oxide}\\F_{Poly}\end{bmatrix}=NF\end{aligned}\tag{10}$$

where F is the column vector of the forces, and N the premultiplication row vector, respectively.

The second requirement is the force and strain relation. Each layer will expand or contract by axial force, piezoelectric strain, and bending as follows.

$$\varepsilon_{Top}=\frac{F_{Top}}{(AE)_{Top}}+\frac{t_{Top}}{2r}\tag{11}$$

$$\varepsilon_{PZT}=d_{31}E_{PZT}+\frac{F_{PZT}}{(AE)_{PZT}}+\frac{t_{PZT}}{2r}\tag{12}$$

$$\varepsilon_{Bottom}=\frac{F_{Bottom}}{(AE)_{Bottom}}+\frac{t_{Bottom}}{2r}\tag{13}$$

$$\varepsilon_{Oxide}=\frac{F_{Oxide}}{(AE)_{xide}}+\frac{t_{Oxide}}{2r}\tag{14}$$

$$\varepsilon_{Poly}=\frac{F_{Poly}}{(AE)_{Poly}}+\frac{t_{Poly}}{2r}\tag{15}$$

In this equation, to express piezo in terms of the transverse piezoelectric coefficient, the consecutive equations for piezoelectric matrices (DeVoe et al., 1997) were used. And the d_{33}, the longitudinal piezoelectric property, was ignored because we assumed no change in the thickness of the piezoelectric film since any amount of change was much smaller than that of the length of the cantilevers.

Lastly, the strain compatibility of bending was applied. Adjacent layers will expand or contract in the same amount, so the strain should be the same as follows.

$$\begin{aligned}&\frac{F_{Top}}{(AE)_{Top}}-\frac{t_{Top}}{2r}\\&=d_{31}E_{PZT}\frac{F_{PZT}}{(AE)_{PZT}}+\frac{t_{PZT}}{2r}\end{aligned}\tag{16}$$

$$\begin{aligned}&d_{31}E_{PZT}\frac{F_{PZT}}{(AE)_{PZT}}-\frac{t_{PZT}}{2r}\\&=\frac{F_{Bottom}}{(AE)_{Bottom}}+\frac{t_{Bottom}}{2r}\end{aligned}\tag{17}$$

$$\frac{F_{Bottom}}{(AE)_{Bottom}}-\frac{t_{Bottom}}{2r}=\frac{F_{Oxide}}{(AE)_{Oxide}}+\frac{t_{Oxide}}{2r}\tag{18}$$

$$\frac{F_{Oxide}}{(AE)_{Oxide}}-\frac{t_{Oxide}}{2r}=\frac{F_{Poly}}{(AE)_{Poly}}+\frac{t_{Poly}}{2r}\tag{19}$$

The electric field in the second piezoelectric layer is the only nonzero field. Because electrostriction effects are ignored, a field in a purely dielectric material does not affect the deflection of the micro

cantilever. These equations can be expressed in matrix form,

$$JF-\frac{1}{2r}K-d_{31}M=0 \tag{20}$$

while matrices J, K, M and N are defined as

$$J=\begin{bmatrix} \frac{1}{(AE)_{Top}} & \frac{-1}{(AE)_{PZT}} & 0 & 0 & 0 \\ 0 & \frac{1}{(AE)_{PZT}} & \frac{-1}{(AE)_{Bottom}} & 0 & 0 \\ 0 & 0 & \frac{1}{(AE)_{Bottom}} & \frac{-1}{(AE)_{Oxide}} & 0 \\ 0 & 0 & 0 & \frac{1}{(AE)_{Oxide}} & \frac{-1}{(AE)_{Poly}} \\ 1 & 1 & 1 & 1 & 1 \end{bmatrix} \tag{21}$$

$$K=\begin{bmatrix} t_{Top}+t_{PZT} \\ t_{PZT}+t_{Bottom} \\ t_{Bottom}+t_{Oxide} \\ t_{Oxide}+t_{Poly} \\ 0 \end{bmatrix} \tag{22}$$

$$M=\begin{bmatrix} \boldsymbol{E}_{PZT} \\ -\boldsymbol{E}_{PZT} \\ 0 \\ 0 \\ 0 \end{bmatrix} \tag{23}$$

$$N=\frac{1}{[(EI)_{Top}+(EI)_{PZT}+(EI)_{Bottom}+(EI)_{Oxide}+(EI)_{Poly}]} \cdot\begin{bmatrix} \frac{t_{Top}}{2} & \frac{2t_{Top}+t_{PZT}}{2} & \frac{2(t_{Top}+t_{PZT})+t_{Bottom}}{2} \\ \frac{2(t_{Top}+t_{PZT}+t_{Bottom})+t_{Oxide}}{2} \\ \frac{2(t_{Top}+t_{PZT}+t_{Bottom}+t_{Oxide})+t_{Poly}}{2} \end{bmatrix} \tag{24}$$

where $\boldsymbol{A}$ denotes the cross sectional area of each layer, t the thickness of each layer, and $\boldsymbol{E}_{PZT}$ electric field applied across the PZT layer.

The radius of curvature can be solved by combining Eqs. 10 and 20 as follows.

$$\frac{1}{r}=\frac{2d_{31}NJ^{-1}M}{2-NJ^{-1}K} \tag{25}$$

Using the radius of curvature from Eq. 25, the deflection of the cantilever with a given voltage can be written as

$$\delta_1(x)=x^2\left[\frac{2d_{31}NJ^{-1}M}{2-NJ^{-1}K}\right] \tag{26}$$

where δ_1 denotes the tip deflection at the end of the first part.

Assuming same radius of curvature, the angle at the end of the first part cantilever can be written as

$$\phi_1(x)=x\left[\frac{4d_{31}NJ^{-1}M}{2-NJ^{-1}K}\right] \tag{27}$$

The resultant tip displacement can be obtained by superposing δ_1 and the deflection by the angle ϕ_1,

$$\delta=\delta_1+L_2\sin(\phi_1) \tag{28}$$

The transverse piezoelectric coefficient was obtained using Eq. (29).

$$d_{31}=e_{31}s_{11}^{E} \tag{29}$$

where, e_{31} is the piezoelectric coefficient. The reciprocal of the Young's modulus is the elastic compliance s_{11}. The dimensions and material properties of the micro cantilever are listed in Table 1. The piezoelectric coefficient of the PZT films on a Si substrate that we used was from -4.1 to -6.0 C/m^2 as applied voltages increased from 1 V to 15 V (Kanno et al., 2003). The calculated

Table 1 Dimensions and mechanical properties of the micro cantilever

Layer	Lenth (μm)	Width (μm)	Thickness (μm)	Young's modulus (N/m^2) (DeVoe et al., 1997)
Top Pt/Bottom Pt	380.00	150.00	0.15	2.50×10^{11}
PZT	380.00	150.00	0.50	1.32×10^{11} (Ryu et al., 2004)
Nitride	450.00	300.00	0.20	2.90×10^{11}
Poly-Si	450.00	300.00	2.00	1.62×10^{11}

Table 2 Deflection of the micro cantilever

Voltage (V)	Analytic solutions (μm)
1	2.76
2	5.62
3	8.57
4	11.61
5	14.75
6	17.99
7	21.31
8	24.74
9	28.25
10	31.86
11	36.10
12	40.00
13	43.90
14	47.90
15	52.00

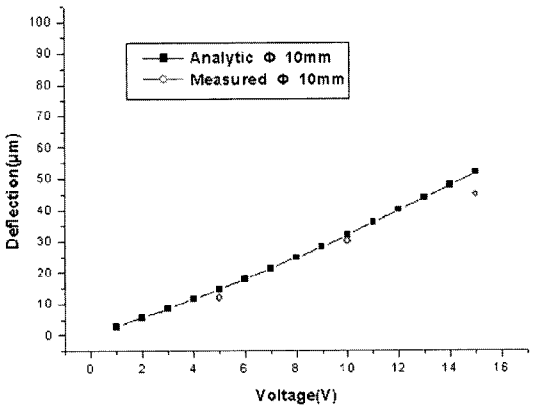

Fig. 7 Tip deflections of the microvalve as a function of applied voltages

deflections was 14.8 μm, at 5 V applied. Tip deflections of the micro cantilever as a function of the applied voltage are shown in Table 2 and Fig. 7.

3. Experimental Results

We fabricated the micro cantilever array on the SIMOX (Separation by ion implantation of oxygen) wafer. SIMOX wafer has an implanted 0.15 μm thick oxide layer on the 4 inch Si wafer. The thickness of Poly-Si layer was 2 μm. The fabrication processes are illustrated in Fig. 8. LPCVD low-stress silicon nitride layer was deposited to a

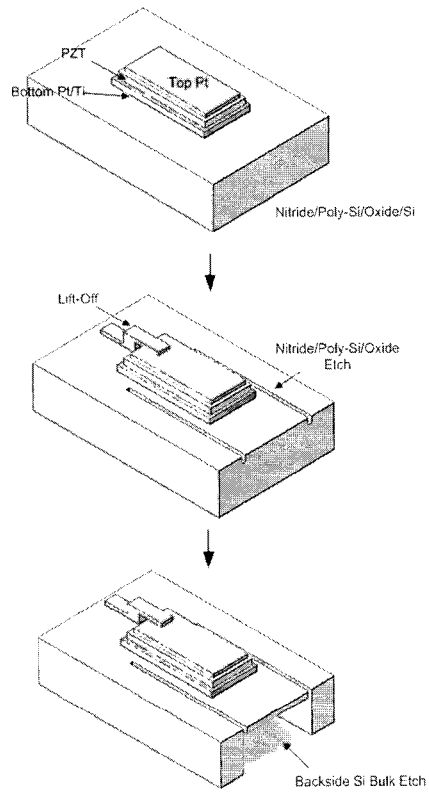

Fig. 8 Fabrication process of a micro cantilever

thickness of 0.4 μm at 835℃ and 150 mTorr with dichlorosilane (SiH_2Cl_2) 100 sccm and NH_3 180 sccm by low pressure chemical vapor deposition (LPCVD). Then 0.03 μm thick titanium (Ti) layer was deposited as an adhesive layer between the platinum (Pt) layer and the nitride layer.

After deposition of the Ti layer, Pt layer for the bottom electrode was deposited by sputtering up to 0.15 μm thickness. On the bottom layer, PZT film was coated up to a thickness of 0.5 μm by the sol-gel method. The sol-gel deposition method is popular because it is compatible with the photolithography process, and it allows precise control of the composition. Furthermore, it can be carried out at relatively low temperature and can coat the PZT film on large area. The precursor composition for PZT film was Pb : Zr : Ti=110 : 52 : 48. This composition provides good piezoelectric and ferroelectric properties. The precursor was then spin coated on the nitride layer deposited SIMOX wafer at 3800 rpm for 25 seconds. The wafer was

then baked on a hot plate at 350℃ for 7 minutes and 430℃ for 6 minutes in a furnace to remove the solvent. After repeating this process 6 times, we could obtain PZT film of 0.5 μm thickness with a smooth and crack-free surface. The PZT film was annealed to crystallize the amorphous film through rapid thermal annealing (RTA). After RTA process at 700℃ for 5 minutes, we could obtain a perovskite structure. The top Pt electrode was sputtered up to 0.10 μm.

Pt/PZT/Pt/Ti layers were patterned by RIE (Reactive Ion Etching) process. The Pt layer was patterned with Cl_2 plasma over a photo-resist mask, which was removed after etch step with O_2 plasma, at a flow rate of 200 sccm and power of 300 W for 10 minutes. The applied bias of the Cl_2 plasma was 300 V. PZT was patterned by RIE in Cl_2/BCl_3 plasma by using a photo-resist mask, which was also removed with the same ashing process. Then, the bottom Pt/Ti layers were etched together with Cl_2 plasma over a photo-resist mask. After this etch process, we could observe the nitride layer that had been laid under the Ti layer. In every etch step, each layer was etch under 20% over-etch condition, and three different mask designs were utilized to clearly isolate the top electrode from the bottom electrode.

In the next step, the gap of cantilever shapes was patterned. The Si_3N_4 layer was patterned by MERIE (Magnetically Enhanced Reactive Ion Etching) with CF_4, CHF_3, O_2 and Ar at flow rates of 10, 15, 10 and 8 sccm, respectively. The applied RF power was 600 W. Then, the poly-Si layer was etched by ICP (Inductively Coupled Plasma) with Cl_2, He, and O_2 gases at a rate of 100, 8 and 10 sccm, respectively. The RF power was 300 W. The buried oxide layer was also etched by MERIE with CF_4, CHF_3, and Ar at rates of 25, 5, and 70 sccm respectively. For each etch step, PR mask was used as the etching mask.

Another Pt layer was sputtered to a thickness of 0.20 μm to pattern the angle shape bridge. In advance, via holes were patterned by using PR through photolithography process. To create good contact between the bridge patterns and the bottom electrode, 1.70 μm PR was developed for seven minutes. The bridge Pt patterns were etched by the same procedure that was used in the patterning of the electrode Pt layer. The remaining PR was also ashed under the same condition.

After finishing the front side patterning, we etched the bulk Si of the backside by ICP (Inductively Coupled Plasma) with C_4F_8, SF_6 and Ar gas plasma at rates of 0.5, 100, and 30 sccm, respectively. The applied RF power was 825 W. The etch stop layer was a 0.15 μm thick SiO_2 layer, which was relatively thin for this bulk etch. So the etch was performed carefullyand the remaining Si thickness was checked after each etch step. The 525 bulk Si was etched successfully with PR etching mask. Wafer can break during this process, so we attached a bare Si wafer on the main wafer for protection. And it was separated after the bulk etch process.

PZT films were characterized with Precision Pro (Radiant Technologies Inc.). We measured the polarization-applied voltage hysteresis loop as shown in Fig. 9. The variation of dielectric constant and dielectric loss versus applied voltages was measured with Impedance Analyzer 4294 (Agilent). The result is shown in Fig. 10.

The dielectric constant decreased from 1300 to 200 as the applied voltage changed from 2 V to 15 V. The dielectric loss was less than 0.05 and decreased from 0.05 to 0.01 as the voltage changed from 2 V to 15 V.

The fabricated micro cantilever arrays are shown in Fig. 11, which were taken by SEM. The cantilevers were actuated with applied voltages from 5 V to 15 V. Tip deflections were measured

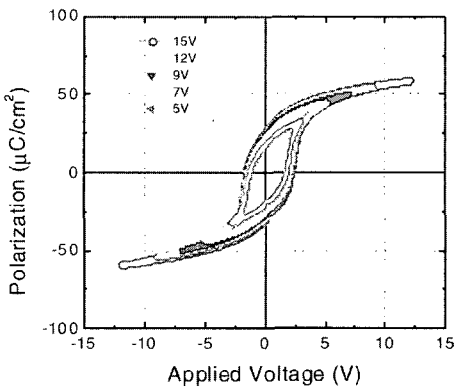

Fig. 9 P-V hysteresis loop of PZT film

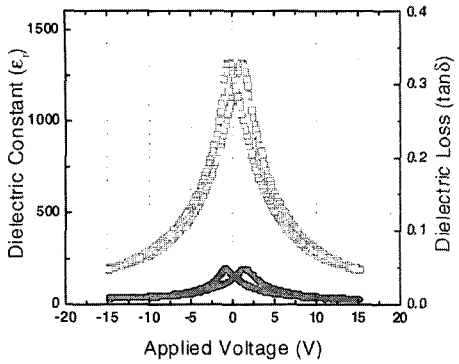

Fig. 10 Dielectric constant, dielectric loss of the PZT film

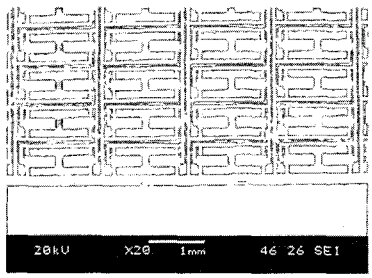

(a)

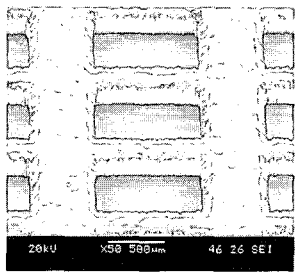

(b)

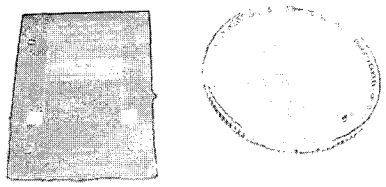

(c)

Fig. 11 Fabricated micro cantilevers array (a) SEM picture of front view, (b) SEM picture of backside view and (c) overall view picture

by laser interferometer. The tip displacements

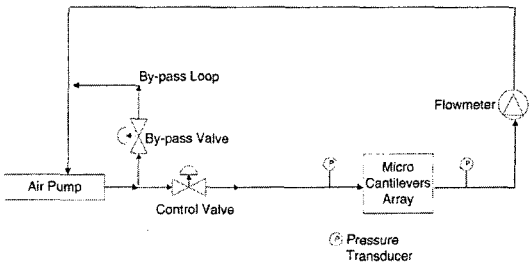

Fig. 12 Test bench configuration

were proportional to the input voltages. The measured tip displacements were 12 μm, 30 μm, and 45 μm at 5 V, 10 V and 15 V, respectively. These values agreed well with the values of 14.8 μm, 32 μm, and 52 μm from the evaluation.

Leakage test was performed with an air pump. The configuration of the test bench is shown in Fig. 12. Pressure differences and flow rates were measured by pressure sensors (PTAAC010KGAG, PMHA-1-10 KAAB, Sensor System Technology Co.,Ltd, South Korea) and a flow meter (EL-FLOW F-110C MFM, Bronkhorst High-Tech BV, The Netherlands), respectively. The measured air flow rate was 18 μl/s at a pressure difference of 1000 Pa.

4. Discussion

Micro cantilevers array showed good performance because they operated at relatively low operating voltages. The outstanding features were ultra slim thickness, and good controllability and compatibility with MEMS fabrication process. Micro cantilevers arrays were applied to a micro cooler. The conceptual design of a micro cooler is shown in Fig. 13. It has five major layers from the top : a condenser, an insulation layer, a compressor with an expansion nozzle, another insulation layer, and an evaporator. The size of the micro cooler is only $\Phi 10 \times 5$ mm, so it can be easily installed on electronics chips. It can remove a heat up to 60 W from the electronics chips. The heat will be transferred to the heat spreader through the heat pipe and will be rejected to the ambient air. The important layer in the micro cooler is the micro compressor layer. Conventional micro motors or PZT actuators cannot

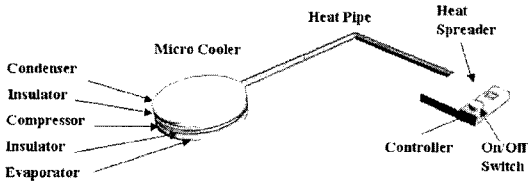

Fig. 13 Conceptual design of a micro cooler

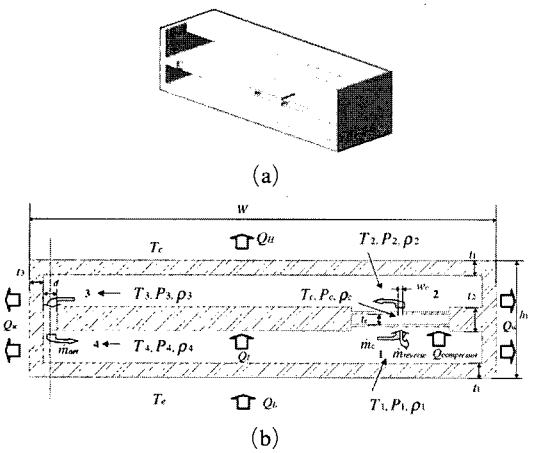

Fig. 14 (a) Isometric view and (b) cross-sectional view of a micro compressor prototype

actuate the compressor. Only the micro cantilevers arrays can actuate the micro compressor.

We developed a prototype of this micro compressor by using a micro cantilevers array, that will modify the conceptual design. This prototype is composed of two micro cantilevers arrays, which are shown in Fig. 14. The upper and lower micro cantilevers arrays are bonded to become a compressor. The working principle is illustrated in four steps in Fig. 15. First, the lower micro cantilevers are deflected downward ; this is the opening process. Second, the upper micro cantilevers are opened upward to maximize the volume of the chamber. Third, the lower micro cantilevers are closed ; this causes the continuous movement of the working fluid upward. Finally, the cycle ends as the upper micro cantilevers closes and push out the fluid. The working fluid flows as this procedure repeats continuously. If the volume of the upper micro channel is smaller than that of the lower one, the fluid is compressed.

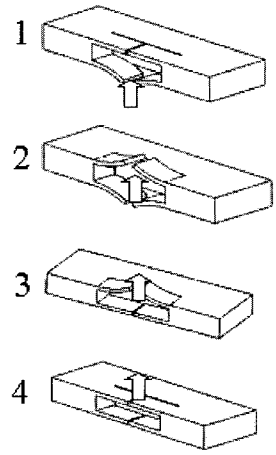

Fig. 15 Working principle of the micro compressor prototype

5. Conclusions

Micro cantilevers arrays for fluidic system were designed and fabricated. A gap designed to 450 μm showed 18 μl/s reverse air leakage at a pressure difference of 1000 Pa. The arrays showed large tip displacement because the cantilever (450 μm$\times$300 μm) was large. The tip deflections were measured for different voltages from 1 V to 15 V. The measured values of deflection at 5 V, 10 V, and 15 V were 12 μm, 30 μm, and 45 μm, which were in good agreementwith the calculated values of 15 μm, 32 μm, and 52 μm, respectively. We will proceed to develop the micro cooler using this micro cantilever array. It will be applied to develop the micro compressor prototype.

Acknowledgments

This research was supported by Micro Thermal System Research Center at Seoul National University.

References

DeVoe, D. L. and Pisano, A. P., 1997, "Modeling and Optimal Design of Piezoelectric Cantilever Microactuators," *Journal of Microelectromechanical Systems*, Vol. 6, pp. 266~270.

Du, L., Kwon, G., Arai, F., Fukuda, T.,

Itoigawa, K. and Tukahara, Y., 2003, "Structure Design of Micro Touch Sensor Array," *Sensors and Actuators A : Physical*, Vol. 107, pp. 7~13.

Flynn, A. M., Tavrow, L. S., Bart, S. F., Brooks, R. A., Ehrlich, D. J., Udayakumar, K. R. and Cross, L. E., 1992, "Piezoelectric Micromotors for Microrobots," *Journal of Microelectromechanical Systems*, Vol. 1, pp. 44~51.

Galassi, C., Dinescu, M., Uchino, K. and Sayer, M., 1999, *Piezoelectric Materials : Advances in Science, Technology and Applications*, Kluwer Academic Publishers.

Itoh, T., Lee, C., Sasaki, G. and Suga, T., 1996, "Sol-gel Derived PZT Force Sensor for Scanning Force Microscopy," *Materials Chemistry and Physics*, Vol, 44, pp. 25~29.

Kanno, I., Kotera, H. and Wasa, K., 2003, "Measurement of Transverse Piezoelectric Properties of PZT Thin Films," *Sensors and Actuators A : Physical*, Vol. 107, pp. 68~74

Kim, C. and Koo, K., 2002, "Development of a PZT Fiber/Piezo-polymer Composite Actuator with Interdigitated Electrodes," KSME International Journal, Vol. 16, No. 5, pp. 666~675.

Kim, D., Kim, B. and Park, J., 2004, "Implementation of a Piezoresistive MEMS Cantilever for Nanoscale Force Measurement in Micro/Nano Robotic Applications," *KSME International Journal*, Vol. 18, No. 5, pp. 789~797.

Koch, M., Harris, N., Evans, A. G. R., White, N. M. and Brunnschweiler, A., 1998, "A Novel Micromachined Pump Based on Thick-Film Piezoelectric Actuation," *Sensors and Actuators A : Physical*, Vol. 70, pp. 98~103.

Kueppers, H., Leuerer, T., Schnakenberg, U., Mokwa, W., Hoffmann, M., Schneller, T., Boettger, U. and Waser, R., 2002, "PZT Thin Films for Piezoelectric Microactuator Applications," *Sensors and Actuators A : Physical*, Vol. 97-98, pp. 680~684.

Lee, S. S. and White, R. M., 1998, "Piezoelectric cantilever voltage-to-frequency converter," Sensors and Actuators A : Physical, Vol. 71, pp. 153~157.

Nam, Y. and Sasaki, M., 2002, "Strain rate self-sensing for a cantilevered piezoelectric beam," KSME International Journal, Vol. 16, No. 3, pp. 310~319.

Ryu, W. H., Chung, Y. -C., Choi, D. -K., Yoon, C. S., Kim, C. K. and Kim, Y. -H., 2004, "Computer Simulation of the Resonance Characteristics and the Sensitivity of Cantilever-Shaped Al/PZT/RuO2 Biosensor," *Sensors and Actuators B : Chemical*, Vol. 97, pp. 98~102.

Yamashita, K., Katata, H., Okuyama, M., Miyoshi, H., Kato, G., Aoyagi, S. and Suzuki, Y., 2002, "Arrayed Ultrasonic Microsensors with High Directivity for in-air Use Using PZT Thin Film on Silicon Diaphragms," *Sensors and Actuators A : Physical*, Vol. 97-98, pp. 302~307.